Available online at www.sciencedirect.com
SCIENCE DIRECT®
Journal of Organometallic Chemistry 689 (2004) 2138–2143
Journal of Organometallic Chemistry
www.elsevier.com/locate/jorganchem

Reverse saturable absorption of lanthanide bisphthalocyanines and their application for optical switches

Mark O. Liu [a], Chia-Hon Tai [b], Andrew Teh Hu [a,*], Tai-Huei Wei [c]

[a] *Department of Chemical Engineering, National Tsing-Hua University, 101, Kuang Fu Rd, Sec.2, Hsinchu 30043, Taiwan, ROC*
[b] *Union Chemical Laboratories, Industrial Technology Research Institute, Hsinchu 300, Taiwan, ROC*
[c] *Department of Physics, National Chung-Cheng University, Chia-Yi, Taiwan, ROC*

Received 2 January 2004; accepted 2 April 2004

Abstract

We have investigated reverse saturable absorption (RSA) of tetrakis(2,9,16,23-*tert*-butyllanthanide bisphthalocyanines)($M(TBPc)_2$, M = Lu, Dy, Tb) with *Z*-scan technique. Furthermore, lanthanide bisphthalocyanines have also been utilized for optical switches based on their RSA performance. However, the experimental results reveal that the performances of RSA and optical switches for $M(TBPc)_2$ (M = Lu, Dy, Tb) are poorer than that of tetrakis(2,9,16,23-*tert*-butylcopper phthalocyanines) (Cu(TBPc)) due to strong intramolecular π–π interaction between the two Pc rings.

Keywords: Optical switch; Bisphthalocyanine; Reverse saturable absorption; *Z*-scan; Optical limiting

1. Introduction

Lanthanide bisphthalocyanines ($LnPc_2$) are well-known electronic materials due to their unusual electrochemical behaviors [1] and have been applied in electrochromic displays [2,3] as well as gas sensors [4]. Recently, metallophthalocyanines (MPc) are found to exhibit reverse saturable absorption (RSA)[5], which can effectively limit the output energy of incident light, and are used for optical switches [6]. However, the RSA of $LnPc_2$ and their application for optical switches have never been reported.

In this paper, the RSA of tetrakis(2,9,16,23-*tert*-butyllanthanide bisphthalocyanines) ($M(TBPc)_2$, M = Lu, Dy, Tb) have been investigated by *Z*-scan technique. Moreover, they are also used for the optical switches based on their RSA by two different laser sources as pump beam and probe beam, respectively. We have also observed the intramolecular π–π interaction between the two Pc rings for $M(TBPc)_2$, which leads to the attenuation of RSA in the triplet state.

* Corresponding author. Tel.: +886-3-5713830; fax: +886-3-5715408.
E-mail address: athu@che.nthu.edu.tw (A. Teh Hu).

2. Experimental

2.1. Preparation of materials

Tetrakis(2,9,16,23-*tert*-butyllanthanide bisphthalocyanines) ($M(TBPc)_2$, M = Lu, Dy, Tb) and tetrakis (2,9,16,23-*tert*-butylcopper phthalocyanine) were synthesized by the procedure reported previously [7]. Their chemical structures were shown in Fig. 1.

2.2. Z-scan measurements

As shown in Fig. 2, *Z*-scan technique was utilized for the toluene solutions of $M(TBPc)_2$ (M = Lu, Dy, Tb) and Cu(TBPc). This technique, which based on intensity (*I*, energy per area per time) attenuation of a Gaussian laser beam after nonlinearly interacting with the samples located at various positions along the beam propagation direction (*z*), has been described before [8]. The transmittance (transmitted energy divided by the input energy) was recorded as a function of *z*.

In this paper, we executed the *Z*-scan experiments with a continuous-wave green laser of 532 nm (50 mW). All of the solution samples were prepared to have the

0022-328X/$ - see front matter © 2004 Elsevier B.V. All rights reserved.
doi:10.1016/j.jorganchem.2004.04.003

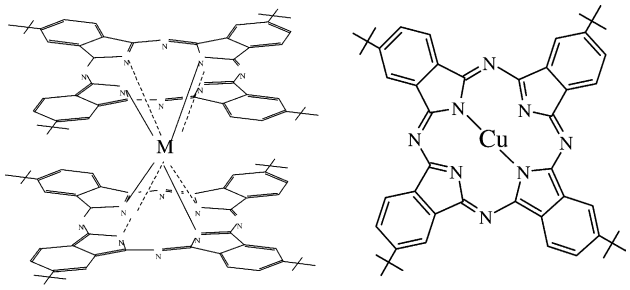

Fig. 1. The chemical structures of lab-made tetrakis(2,9,16,23-*tert*-butyllanthanide bisphthalocyanines ($M(TBPc)_2$, M = Lu, Dy, Tb) and tetrakis(2,9,16,23-*tert*-butylcopper phthalocyanine (Cu(TBPc)).

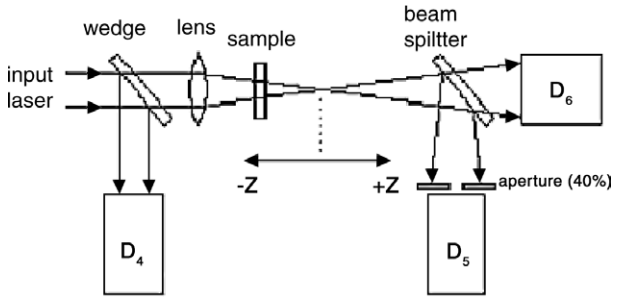

Fig. 2. The instrument of *Z*-scan. D_4, D_5, and D_6 are detectors.

concentration of 10^{-4} M in toluene and contained in a 1 mm quartz cell.

2.3. Setup of optical switch

The optical switch for $M(TBPc)_2$ (M = Lu, Dy, Tb) and Cu(TBPc) was shown in Fig. 3. We utilized continuous-wave green laser of 532 nm (50 mW) and H_2–Ne red laser of 632 nm (5 mW) as pump beam and probe beam, respectively. The probe and pump beam firstly passed through half-wavelength plates and polarizers. After reflected by the reflective mirrors, they were focused by a convex–plano lens and passed through the sample. The chopper, 5, was maneuvered by the controller and could cut off the passing of the pump beam. Finally, the passing beams were filtrated by a filter of 632 nm. The intensity of output beam was detected by a photodiode and then the data was transmitted to the oscillator.

3. Results and discussion

3.1. RSA properties

As shown in Fig. 4, $M(TBPc)_2$ (M = Lu, Dy, Tb) exhibit two characteristic absorptions [9,10], which are B

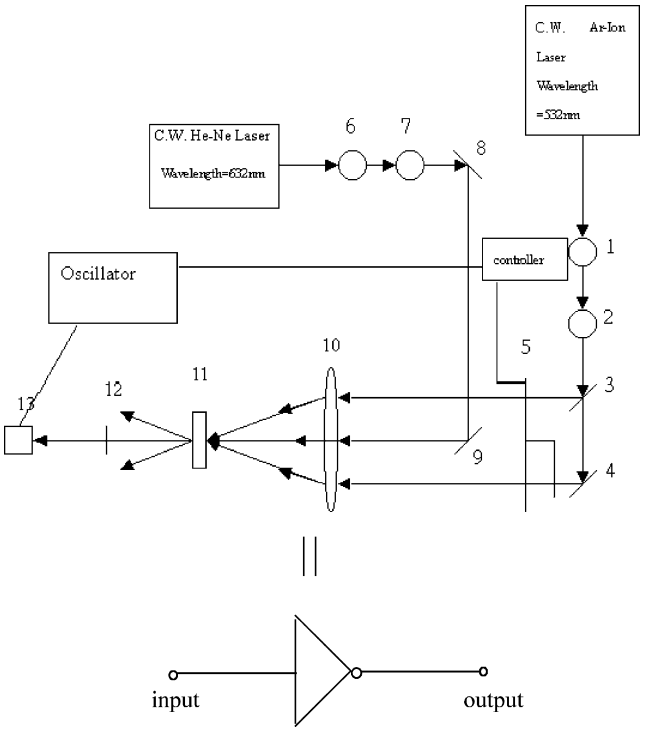

Fig. 3. The setup of optical switch (1: half-wavelength plate (532 nm); 2,7: polarizer (range: 350–2500 nm); 3: beamsplitter (532 nm, anti-reflection = 45%); 4,8,9: reflective mirror coated with aluminum; 5: chopper; 6: half-wavelength plate (632 nm); 10: convex–plano len (f = 12.5 cm); 11: sample; 12: filter (632 nm); 13: photodiode). The optical switch is a NOT gate.

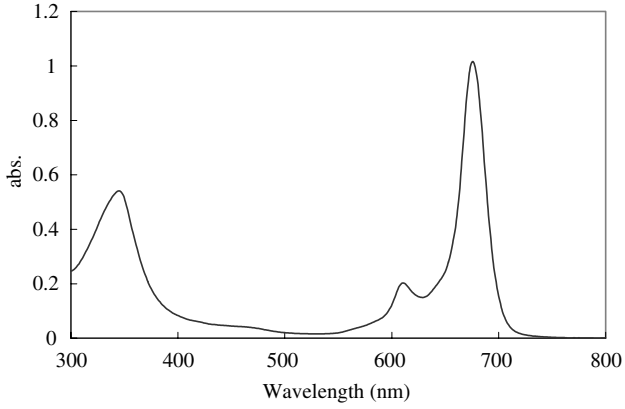

Fig. 4. The UV/Vis spectrum of $Lu(TBPc)_2$ in toluene.

band (300–400 nm) and Q band (600–800 nm), respectively, because of $S_0 \rightarrow S_1$ and $S_0 \rightarrow S_2$ transitions. The interesting region of optical limiting effect for bisphthalocyanine molecules lies in the highly transparent regime between 450 and 550 nm. Consequently, we focused the region near 532 nm for instrumental consideration.

Optical excitation of our samples can be described with the five-energy-state scheme [11]. As shown in Fig. 5, each band, including the associated zero-point

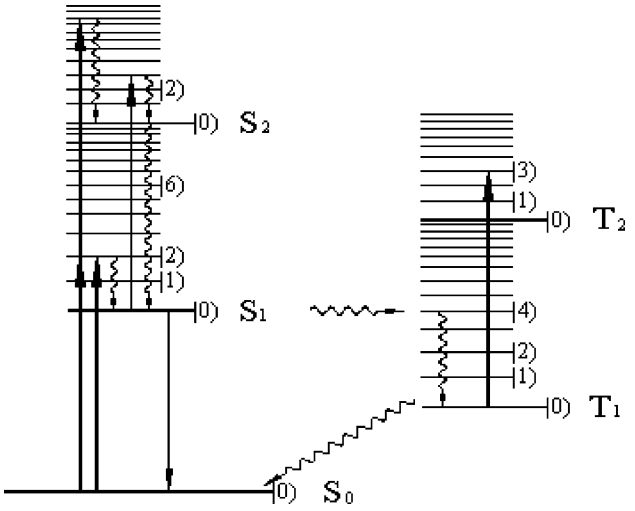

Fig. 5. The five-energy-state scheme of $M(TBPc)_2$. Upward-pointing arrows, wiggly lines, and downward-pointing arrows represent optical excitation, non-radiative relaxation, and radiative relaxation, respectively. $|v\rangle$ are the vibrational eigenstates involved in the transitions.

level $|0\rangle$ and vibronic level $|v \neq 0\rangle$, is named as S_m for the singlet manifold and T_m for the triplet manifold where subscript m refers to the state formed from certain electronic configurations in molecular orbitals. At thermal equilibrium, all the molecules π free electrons reside on the ground state ($S_0(\pi)$). Pumped by laser pulses of 532 nm, some of them are excited to $|v\rangle S_1$ by one-photon absorption or to $|v\rangle S_2$ via two-photon absorption. Those promoted to $|v\rangle S_1$ first relax to the zero point level $|0\rangle$ and then undergo one of the following process: (i) decay to ground state radiatively (fluorescence) or nonradiatively (internal conversion); (ii) intersystem crossing (τ_{isc}, with a time constant); (iii) one-photon excitation to S_2. The Beer's law equation can be written as

$$\frac{dI}{dz'} = -\alpha I = -[\sigma_{S0}N_{S0} + \sigma_{S1}N_{S1}]I - \beta N_{S0}I^2. \quad (1)$$

In Eq. (1), σ and N, respectively represent the absorption cross-section and molecular concentration of the states specified by the subscripts.

Associated with Eq. (1), the population change rates are

$$\frac{dN_{S0}}{dt} = -\frac{\sigma_{S0}N_{S0}I}{\hbar\omega} - \frac{\beta N_{S0}I}{2\hbar\omega}, \quad (2)$$

$$\frac{dN_{S1}}{dt} = \frac{\sigma_{S0}N_{S0}I}{\hbar\omega} + \frac{\beta N_{S0}I^2}{2\hbar\omega} - \frac{\sigma_{S1}N_{S1}I}{\hbar\omega} + \frac{N_{S2}}{\tau_{S2}} \quad (3)$$

and

$$\frac{dN_{S2}}{dt} = \frac{\sigma_{S1}N_{S1}I}{\hbar\omega} - \frac{N_{S2}}{\tau_{S2}}, \quad (4)$$

where $\hbar$ represents the Planck constant divided by 2π and ω is the frequency of laser. At very low input intensity, α equals $\sigma_{S0}N_{S0}(-\infty)$.

When $\sigma_{S1} > \sigma_{S0}$ (σ_{S1}: absorption cross-section of excited state; σ_{S0}: absorption cross-section of ground state), as explained in [12], α increases as I increases and thus the sample shows RSA. When $\sigma_{S1} < \sigma_{S0}$, α decreases as I increases and thus the sample shows SA. When $\sigma_{S1} = \sigma_{S0}$, α is a constant and thus the sample shows linear absorption.

As shown in Fig. 6, the Z-scan results were numerically fitted with Eqs. (1)–(4). The best fits (solid lines in Figures) were obtained with the values of σ_{S1} shown in Table 1. σ_{S0} is derived from α based on Eq. (5)–(7) while α was measured in the linear region of the Z-scan apparatus

$$\frac{dI}{dz'} = -\alpha I, \quad (5)$$

where z' is the penetration of the light into the sample

$$T \equiv \frac{I_l}{I_0} = e^{-\alpha l}, \quad (6)$$

where I_l represents the intensity at the rear surface of the sample and l denotes the sample thickness of sample

$$A \equiv \log\frac{1}{T} = \varepsilon C l, \quad (7)$$

where ε is the proportional constant (extinction coefficient) and C is the concentration of sample. We can integrate Eqs. (6) and (7) to obtain $\alpha = 2.303\varepsilon C$. Finally, σ_{S0} can be obtained by Eq. (8)

$$\alpha = N_{S0}\sigma_{S0} = 6.02 \times 10^{23} \times \frac{C}{1000} \times \sigma_{S0}. \quad (8)$$

The σ_{S1}/σ_{S0} values of $M(TBPc)_2$, which can evaluate the performance of optical limiting, were also summarized in Table 1. All of them were larger than 1. This

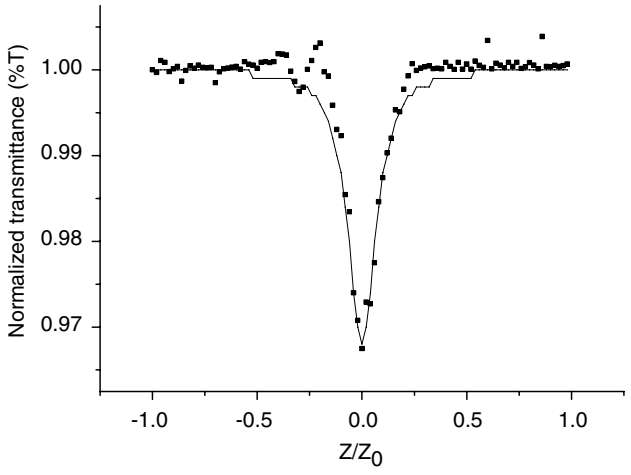

Fig. 6. Open aperture Z-scan results of $Lu(TBPc)_2$ in toluene. The input intensity is 1 μJ. Triangle represents experimental data and solid line for theoretical fits. z is the beam propagation direction. z/z_0 is defined to be normalized distance from focus to sample (e.g., $z/z_0 = 0$ represents the sample locates in the focus. $z/z_0 = +1$ or 1 represents the sample locates in the maximum edge) as shown in Fig. 2.

Table 1
The parameters of RSA and optical switches for lab-made $M(TBPc)_2$ and Cu(TBPc)

Compound	α (cm^{-1})	ε (l mol^{-1} cm^{-1})	σ_{S0} (cm^2)	σ_{S1}[a] (cm^2)	σ_{S1}/σ_{S0}	Response time for optical switch (ms)
$Lu(TBPc)_2$	0.33	1432	5.48×10^{-18}	1.15×10^{-17}	2.1	1.40
$Tb(TBPc)_2$	0.34	1500	5.73×10^{-18}	1.75×10^{-17}	3.1	1.84
$Dy(TBPc)_2$	2.30	10 000	3.82×10^{-17}	4.5×10^{-17}	1.2	1.92
Cu(TBPc)	0.2891	1255	4.8×10^{-18}	14.1×10^{-17}	29.4	1.28

[a] The data are measured by the excitation at 532 nm.

reveals that the absorption cross-sections of excited state for $M(TBPc)_2$ are larger than those of ground state, and $M(TBPc)_2$ are exhibiting RSA properties. While RSA takes place, the electrons in the singlet excited state can absorb the energy of laser to hop to higher-order singlet excited states. Since the duration of electrons in the singlet excited state extend, the probability of intersystem crossing increase. While RSA does not take place, the electrons in the singlet excited state cannot absorb the energy of laser to hop to higher-order singlet excited states and easily decay to the ground state. Therefore, RSA leads to the efficient intersystem crossing.

In comparison with Cu(TBPc), however, the σ_{S1}/σ_{S0} values of $M(TBPc)_2$ are much less than that of Cu(TBPc) due to the strong intramolecular π–π interaction between the two Pc rings for $M(TBPc)_2$ [13]. The strong intramolecular π–π interaction increases relaxation routes and therefore decreases the triple-state lifetime [13]. This suppresses the triplet-state absorption with diminishing the triplet-state population accumulation.

3.2. Optical switch

The absorptions of triple state for $M(TBPc)_2$ at 632 nm are much larger than those of singlet state [6], causing the diversity of intensity for output probe beam. While $M(TBPc)_2$ exhibit RSA, the electrons can be excited to triplet state via intersystem crossing and the intensity of output probe beam is low because of high absorption. However, the population of triplet state decreases and the intensity of output probe beam is high if $M(TBPc)_2$ do not exhibit RSA. The high and low values of intensity for output probe beam can be defined as "0" and "1", respectively. Based on this, we designed an optical switch with $M(TBPc)_2$ as shown in Fig. 3.

When the chopper was on (defined as "1"), the pump beam of 532 nm could pass through the sample and pump the electrons of ground state to the triplet state. Since the absorption of triplet state was high at 632 nm [6], the intensity of output probe beam was low (defined as "0"). When the chopper was off (defined as "0"), the pump beam cannot pass through the sample and the population of triplet state decreased. In this case, the intensity of output probe beam was high (defined as "1") because of low linear absorption at 632 nm. Its performance behaves as an optical switch. In fact, as shown in Figs. 7–10, the optical switch is a NOT gate [14] since the output is always the opposite of the input (input "0" → output "1" and input "1" → output "0").

As shown in Table 1, $Lu(TBPc)_2$ exhibits the shortest response time, which is defined as the period of output signals in Figs. 7–10, among lab-made $M(TBPc)_2$. Since $Lu(TBPc)_2$ has bigger central metal (Lu) than $Tb(TBPc)_2$ and $Dy(TBPc)_2$, its spin–orbit coupling parameter is higher [15] and the speed of intersystem crossing escalates. Therefore, the density of electrons accumulated in the triple state increases when the chopper is on and the pump beam passes through it. Meanwhile, it performs RSA and the electrons in the triplet state can absorb the energy of probe beam to hop to higher level more quickly, causing the intensity of output probe beam drops more rapidly. We speculate that this is the reason why the response time of $Lu(TBPc)_2$ is the shortest among lab-made $M(TBPc)_2$. Nevertheless, compared with Cu(TBPc), the response time of $M(TBPc)_2$ are longer than that of Cu(TBPc) as shown in Table 1 because the strong intramolecular π–π interaction reduces the triplet-state population accumulation and slow down the triplet-state absorption at

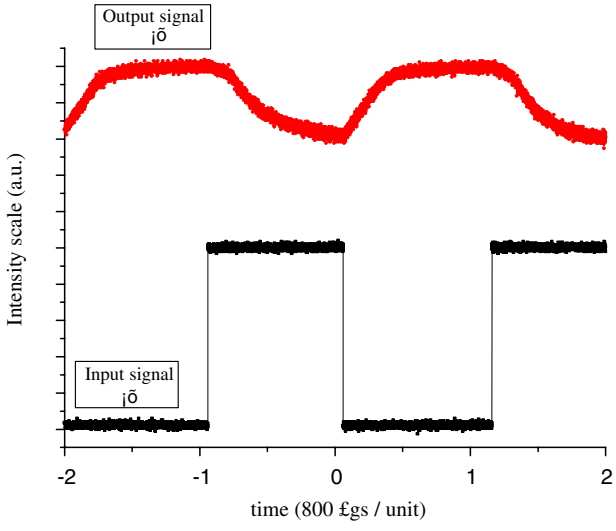

Fig. 7. The signal of optical switch for $Lu(TBPc)_2$. The input signal represents the signal of chopper. The higher value represents that the chopper is "on" and the pump beam can pass through the sample. The lower value represents that the chopper is "off" and the pump beam cannot pass through the sample. The output signal represents the intensity of output probe beam.

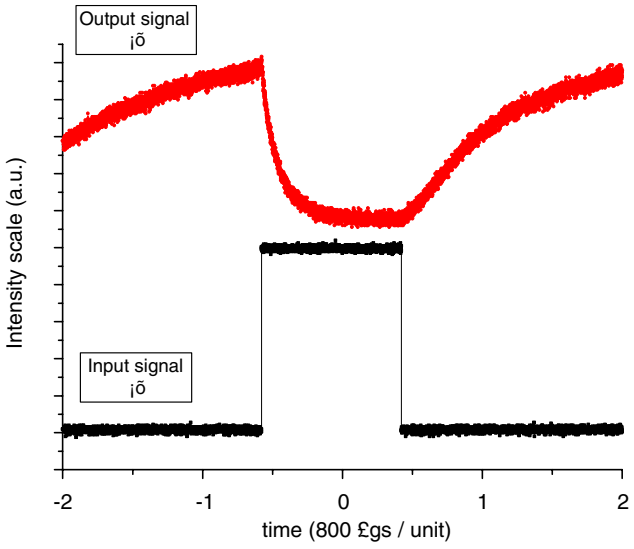

Fig. 8. The signal of optical switch for $Tb(TBPc)_2$. The input signal represents the signal of chopper. The higher value represents that the chopper is "on" and the pump beam can pass through the sample. The lower value represents that the chopper is "off" and the pump beam cannot pass through the sample. The output signal represents the intensity of output probe beam.

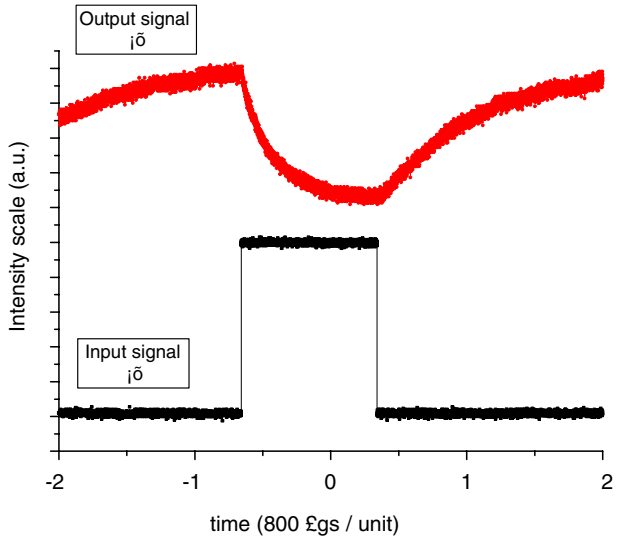

Fig. 9. The signal of optical switch for $Dy(TBPc)_2$. The input signal represents the signal of chopper. The higher value represents that the chopper is "on" and the pump beam can pass through the sample. The lower value represents that the chopper is "off" and the pump beam cannot pass through the sample. The output signal represents the intensity of output probe beam.

632 nm. Furthermore, response times of $Tb(TBPc)_2$ and $Dy(TBPc)_2$ are different between on/off and off/on, as shown in Figs. 8 and 9 because fatigue takes place, resulting in longer response time for off/on.

In this study, $M(TBPc)_2$ (double-decker) have been demonstrated to be less suitable candidates for optical switches than M(TBPc) since the strong intramolecular

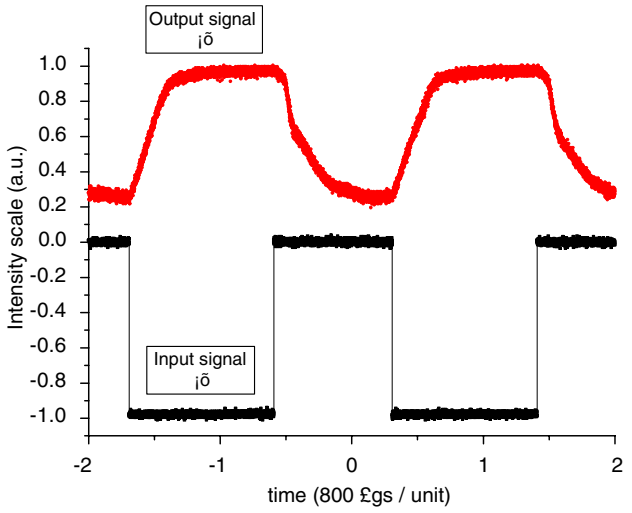

Fig. 10. The signal of optical switch for Cu(TBPc). The input signal represents the signal of chopper. The higher value represents that the chopper is "on" and the pump beam can pass through the sample. The lower value represents that the chopper is "off" and the pump beam cannot pass through the sample. The output signal represents the intensity of output probe beam.

π–π interaction *between the two Pc rings* decreases RSA in the triple state. Moreover, we cannot also measure switch time of the optical switches because the laser used in the experiments was continuous-wave laser. Further improvements to acquire the switch time may utilize pulse laser.

4. Conclusion

The RSA of $M(TBPc)_2$ have been investigated by *Z*-scan technique. Based on their RSA, they are applied for optical switches as a NOT gate with two different laser sources as pump beam and probe beam, respectively. Furthermore, the strong intramolecular π–π interaction for bisphthalocyanines results in that their σ_{S1}/σ_{S0} values are smaller than those of mono-phthalocyanines and their response time of optical switches are longer than those of mono-phthalocyanines.

Acknowledgements

Financial support by the National Science Council of Taiwan for A.T. Hu (NSC-902216E007032) is highly appreciated. We also thank Professor T.H. Wei, National Chung-Cheng University, for instrumental support.

References

[1] A. Iwase, C. Harnoode, Y. Kameda, J. Alloy Compd. 192 (1993) 280.
[2] Y. Liu, K. Shigehara, M. Hara, A. Yamada, J. Am. Chem. Soc. 113 (1991) 440.

[3] L. Gaffo, D. Goncalves, A. Dhanabalan, W.C. Moreira, O.N. Oliveira Jr., Synth. Met. 124 (2001) 351.
[4] D. Xie, W. Pan, Y.D. Jiang, Y.R. Li, Mater. Lett. 57 (2003) 2395.
[5] D.R. Coulter, V.M. Miskowski, J.W. Perry, T.H. Wei, E.W. Van Stryland, D.J. Hagan, SPIE Proc. 1105 (1989) 42.
[6] F.Z. Henari, J. Opt. A: Pure Appl. Opt. 3 (2001) 188.
[7] L.C. Liu, C.C. Lee, A.T. Hu, J. Porphyr. Phthalocya. 5 (2001) 806.
[8] T.H. Wei, T.H. Huandg, T.C. Wen, Chem. Phys. Lett. 314 (1999) 403.
[9] N.B. McKeown, Phthalocyanine Material Synthesis, Structure and Function, Cambridge University Press, Cambridge, 1998, p. 112.
[10] C.C. Leznoff, A.B.P. Lever, Phthalocyanines Properties and Applications, VCH, Cambridge, 1989, p. 146.
[11] T.H. Wei, Tzer-Hsiang Huang, Opt. Quantum Electron. 28 (1996) 1495.
[12] F. Bentivegna, M. Canva, P. Georges, A. Brun, F. Chaput, L. Malier, J.-P. Boilot, Appl. Phys. Lett. 62 (1993) 1271.
[13] X. Wang, C. Liu, Q. Gong, Y. Huang, C. Huang, Opt. Commun. 197 (2001) 83.
[14] J.D. Irwin, D.V. Kerns Jr., Introduction to Electrical Engineering, Prentice-Hall, Inc., Englewood Cliffs, NJ, 1995, p. 250.
[15] J.W. Perry, K. Mansour, S.R. Marder, K.J. Perry, Opt. Lett. 19 (1994) 625.